Dynamical coherent-potential approximation to the magnetism in a correlated electron system

Y. Kakehashi
Max-Planck Institut für Physik komplexer Systeme, Nöthnitzer Strasse 38, D-01187 Dresden, Germany
(Received 27 November 2001; published 29 April 2002)

A dynamical coherent-potential approximation for correlated electron systems has been developed on the basis of a functional integral method and the harmonic approximation that neglects the mode-mode couplings between dynamical potentials. Within the single-site approximation, the theory becomes exact in the high-temperature limit, reproduces the results of the second-order perturbation theory for small Coulomb interaction, and takes into account the terms that are needed to describe the strongly correlated limit. The theory interpolates between the weak Coulomb interaction limit and the atomic limit. An approximation scheme has been developed to implement the numerical calculations. The model calculations have been performed for the electron number $n=1.44$ (bcc) and $n=1.80$ (fcc). In the case of the former, the magnetization vs temperature curve and the Curie-Weiss susceptibility are obtained. It is found that the Curie temperature is reduced by a factor of 2 due to dynamical effects. In the case of the latter, the dynamical effects are found to make the ferromagnetism unstable. In both cases a many-body satellite peak and a band narrowing are found in the paramagnetic density of states for the single-particle excitation energy.

DOI: 10.1103/PhysRevB.65.184420 PACS number(s): 75.10.Lp, 75.50.Bb, 75.50.Cc, 71.10.−w

I. INTRODUCTION

A theory describing the electron correlations from a weak Coulomb interaction to a strong one has intrigued us for a long time because of its basic importance in solid-state physics, as well as our basic interest for a unified understanding of a variety of properties of materials. In the theory of magnetism, such an interpolation theory has been attempted to explain the magnetic properties of transition metals and alloys showing the localized as well as itinerant electron behaviors.[1] For example, the noninteger ground-state magnetization (in units of the Bohr magneton) and the large Sommerfeld coefficient γ in Fe, Co, Ni have been explained by the band model, while their reduced magnetization curves and the Stoner-Wohlfarth ratios (*i.e.*, the ratios of the effective Bohr magneton number to the ground-state magnetization) are close to those expected from the Heisenberg model.

A theory that incorporates the distinct features mentioned above was first proposed by Cyot[2] on the basis of the functional integral method[3,4] and the narrowband model.[5,6] He showed that the functional integral method, in which the interacting Hamiltonian is transformed into one-electron Hamiltonian with time-dependent random fictitious fields, can describe both localized and itinerant features because of its interpolating character. Hubbard[7] and Hasegawa[8] independently established the single-site spin fluctuation theory adopting the coherent-potential approximation[9] (CPA) in the functional integral method. The theory explained qualitatively or semiquantitatively the magnetization vs temperature curves, the Curie temperatures (T_C), the Curie-Weiss susceptibilities as well as the large specific heats at T_C in transition metals and alloys, assuming phenomenological effective Coulomb integrals.

The theories mentioned above are based on the static approximation in the functional integral method, in which the time dependence of the field variables is neglected. The static approximation reduces to the Hartree-Fock one at the ground state. It neglects the ground-state electron correlations that were emphasized to be crucial for the stability of ferromagnetism by Gutzwiller,[5] Hubbard,[6] and Kanamori.[10] Kakehashi and Fulde,[11–13] therefore, developed a variational approach (VA) to the electron correlations at finite temperatures. The theory adiabatically takes into account the Gutzwiller-type local electron correlations[14] that certainly persist over the characteristic temperature range of magnetism. They showed a large reduction of T_C (by a factor of 3 in case of Fe) and strong suppression of charge fluctuation above T_C. Hasegawa[15] developed a similar theory at finite temperatures using the slave-boson functional integral technique.[16] Although the Néel temperatures calculated from the VA and the slave boson functional integral method have recently been verified to be reasonable for the half-filled band by means of the high-temperature expansion technique[17] and the other alternative theories,[18] the entropy in the static approximation remains unimproved because these theories adiabatically take into account the correlation energy at finite temperatures.

Dynamical effects have to be directly taken into account to go beyond the adiabatic approximation. We proposed such a theory called the dynamical CPA.[19] The theory takes into account all the dynamical effects within the single-site approximation and chooses the best surrounding medium by using the CPA. Applying the Monte Carlo sampling technique, we obtained reasonable amplitudes of local moments, the satellite structure in the single-particle excitation spectra, and the Fermi-liquid-like momentum distribution at finite temperatures. Although recent developments of the Monte Carlo method and the other computational techniques[20] have allowed us to calculate various physical quantities accurately, there is still difficulty in calculating magnetic properties at low temperatures, including the Curie temperature.

We propose in the present paper an approximate, but more analytic theory of dynamical CPA adopting the harmonic approximation (HA) to the functional integral technique. The HA, which was proposed by Amit and Bender,[21] and Amit and Keiter,[22] is the neglect of the mode-mode couplings be-

tween dynamical potentials. In spite of its simplicity, the HA holds the following features:

(1) the zeroth harmonic approximation is the static approximation that interpolates between the weak and strong Coulomb interaction limits and has been applied to various problems.[23–26]

(2) The approximation is accurate up to the second order in the Coulomb interaction U when the free energy is expanded with respect to U.

(3) The approximation quantitatively describes the Kondo limit when it is applied to the Anderson model.[27]

(4) The approximation does not depend on the amplitude of spin fluctuations, therefore one may expect that the HA describes large dynamical spin fluctuations as well as small ones.

These features indicate that the HA is one of the suitable approximations for constructing a dynamical interpolation theory.

In the following section, we review the dynamical CPA. Applying the functional integral method, we express the free energy for interacting electrons by means of a time-dependent one-electron Hamiltonian with random spin and charge fictitious fields. We then introduce the coherent potential (*i.e.*, the effective medium), and expand the scattering potential in the effective medium with respect to the site. Neglecting the intersite interactions and choosing the best effective medium, we reach the free energy of the dynamical CPA. In the present paper, we use the free energy that is expressed by the effective potential projected onto the static-field variables. We derive it in the remaining part of Sec. II.

We develop the analytic theory of the dynamical CPA in Sec. III A adopting the harmonic approximation. Integrating the dynamical part over all the finite frequency components of the field variables, we derive the analytic expression of the effective potential, from which we obtain the expressions of various thermodynamic quantities. To implement the numerical calculations, we need further approximations to the dynamical potential. We propose the asymptotic approximation in Sec. III B, which greatly reduces the number of terms to be calculated. The approximation is an approach from the strong Coulomb-interaction limit or the high-temperature limit. It is not easy to cover the weak-interaction region using the asymptotic approximation. We, therefore, propose an interpolation scheme in Sec. III C, which is suitable for both the weak and the strong Coulomb interaction limits.

We present in Sec. IV the numerical examples for the bcc model band with the electron number $n=1.44$ $(=7.2/5)$ which we call Fe, and for the fcc model band with $n=1.80$ $(=9.0/5)$ which we call Ni. We will demonstrate that the dynamical effects reduce the Curie temperature by a factor of 2 in the case of Fe, while the dynamical effects make the ferromagnetism unstable in the case of Ni. The susceptibility and amplitude of local moment are also calculated there, and are compared with those of the static approximation as well as the previous results of calculations based on the VA. Calculated single-particle excitation spectra in the paramagnetic state show a many-body satellite peak and a narrowing of the main band for both cases. A summary and the discussions on the HA are given in Sec. V.

II. DYNAMICAL CPA

We adopt here a narrowband model Hamiltonian with a single orbital, which is given by

$$\hat{H}=\sum_{i,\sigma}(\epsilon_i^0-h_i\sigma)n_{i\nu\sigma}+\sum_{i,j,\sigma}t_{ij}a_{i\sigma}^{\dagger}a_{j\sigma}+\sum_i U_i n_{i\uparrow}n_{i\downarrow}. \tag{1}$$

Here ϵ_i^0, h_i, t_{ij}, and U_i denote the atomic energy level, the local magnetic field, the transfer integral between sites i and j, and the Coulomb integral on site i, respectively. $a_{i\sigma}^{\dagger}(a_{i\sigma})$ is the creation (annihilation) operator for an electron with spin σ on site i, and $n_{i\sigma}=a_{i\sigma}^{\dagger}a_{i\sigma}$ is the number operator for the electron.

In the functional integral method, the free energy $\mathcal{F}$ of the interacting Hamiltonian $\hat{H}$ is transformed into that of the one-electron Hamiltonian $H(\tau,\xi,\eta)$ with time-dependent fictitious random fields $\{\xi_i(\tau),\eta_i(\tau)\}$ acting on each site, by using the Hubbard-Stratonovich transformation.[28,29]

$$e^{-\beta\mathcal{F}}=\int\left[\prod_{i=1}^{N}\delta\xi_i\delta\eta_i\right]\mathrm{Tr}\left(\mathcal{T}\exp\left[-\int_0^{\beta}H(\tau,\xi,\eta)d\tau\right]\right)\times\exp\left[-\frac{1}{4}\sum_i\int_0^{\beta}d\tau U_i[\eta_i(\tau)^2+\xi_i(\tau)^2]\right], \tag{2}$$

$$H(\tau,\xi,\eta)=\sum_{j,\sigma}\left(\epsilon_j^0-\mu-h_j\sigma+\frac{1}{2}iU_j\eta_j(\tau)-\frac{1}{2}U_j\xi_j(\tau)\sigma\right)n_{j\sigma}(\tau)+\sum_{i,j,\sigma}t_{ij}a_{i\sigma}^{\dagger}(\tau)a_{j\sigma}(\tau). \tag{3}$$

Here we adopted the two-field method introducing the spin and charge auxiliary fictitious fields, $\{\xi_i(\tau)\}$ and $\{\eta_i(\tau)\}$. $\int\delta\xi_i$ denotes the functional integral over the imaginary time τ that varies from 0 to β, β being the inverse temperature $1/T$. N is the number of lattice points. $\mathcal{T}$ in the trace is the time ordered product. The operators in the time-dependent Hamiltonian (3) are given in the interaction representation with respect to the noninteracting Hamiltonian $H_0=\Sigma_{i,j,\sigma}t_{ij}a_{i\sigma}^{\dagger}a_{j\sigma}$. Furthermore, μ denotes the chemical potential for electrons.

The Fourier representation of the partition function (2) is given by

$$e^{-\beta\mathcal{F}}=\int\left[\prod_{i=1}^{N}\delta\xi_i\delta\eta_i\right]e^{-\beta E[\xi,\eta]}, \tag{4}$$

$$E[\xi,\eta]=-\beta^{-1}\ln\mathrm{Tr}(e^{-\beta H_0})-\beta^{-1}\mathrm{Tr}\ln(1-vg)+\frac{1}{4}\sum_i\sum_l U_i(|\eta_{il}|^2+|\xi_{il}|^2), \tag{5}$$

$$(v)_{il\sigma jm\sigma'}=v_{\sigma}(i\omega_l-i\omega_m)\delta_{ij}\delta_{\sigma\sigma'}$$
$$\equiv[(\epsilon_i^0-\mu-h_i\sigma)\delta_{lm}+\tfrac{1}{2}U_i(i\eta_{i\ l-m}-\xi_{i\ l-m}\sigma)]\delta_{ij}\delta_{\sigma\sigma'}. \quad (6)$$

Here the Fourier representation of the functional integral is expressed as

$$\int \delta\xi_i\delta\eta_i = \int \sqrt{\frac{\beta U_i}{4\pi}}d\xi_{i0}\sqrt{\frac{\beta U_i}{4\pi}}d\eta_{i0}\left(\prod_{l=1}^{\infty}\frac{\beta U_i}{2\pi}d^2\xi_{il}\frac{\beta U_i}{2\pi}d^2\eta_{il}\right). \quad (7)$$

The variables ξ_{il} (η_{il}) in Eqs. (5)–(7) are the l frequency components of random spin (charge) field $\xi_i(\tau)$ [$\eta_i(\tau)$]. g denotes the Green function matrix for the noninteracting system H_0.

In the effective medium approach,[19] we replace the dynamical potential v in Eq. (5) with the diagonal coherent potential $\Sigma_{j\sigma}(i\omega_l)$, which is independent of the field variables, and expand the remaining part of free energy with respect to the site.

$$\mathcal{F}=\tilde{\mathcal{F}}-\beta^{-1}\ln\int\left[\prod_i \delta\xi_i\delta\eta_i\right]\times\exp\left[-\beta\left(\sum_i E^{(i)}[\xi_i,\eta_i]+\Delta E\right)\right]. \quad (8)$$

Here the zeroth-order term $\tilde{\mathcal{F}}$ is the coherent part of the free energy, which does not depend on any dynamical potentials,

$$\tilde{\mathcal{F}}=-\beta^{-1}\ln \mathrm{Tr}(e^{-\beta H_0})-\beta^{-1}\mathrm{Tr}\ln(1-\Sigma g). \quad (9)$$

The first-order term in Eq. (8) consists of the sum of the single-site energies $\{E^{(i)}[\xi_i,\eta_i]\}$ that only depend on the dynamical potential on the same site,

$$E^{(i)}[\xi_i,\eta_i]=-\beta^{-1}\mathrm{tr}\ln(1-\delta v_i F_i)+\frac{1}{4}\sum_l U_i(|\eta_{il}|^2+|\xi_{il}|^2). \quad (10)$$

Here $\delta v_i=v_i-\Sigma_i$, and tr denotes the trace on a site.

The energy ΔE in Eq. (8) describes the intersite dynamical correlations.

$$\Delta E=-\beta^{-1}\mathrm{Tr}\ln(1-\tilde{t}F')=\sum_{(i,j)}\Phi_{ij}[\xi_i\eta_i,\xi_j\eta_j]+\cdots. \quad (11)$$

The lowest-order term is given by the RKKY-type pair energies $\Phi_{ij}[\xi_i\eta_i,\xi_j\eta_j]$ that are expressed by

$$\Phi_{ij}[\xi_i\eta_i,\xi_j\eta_j]=-\beta^{-1}\mathrm{tr}^{(ij)}\ln(1-\tilde{t}F'). \quad (12)$$

Here $\mathrm{tr}^{(ij)}$ means the trace on sites i and j. Note that their interaction strength is determined by the single-site t-matrix defined by

$$\tilde{t}_i=(1-\delta v_i F_i)^{-1}\delta v_i. \quad (13)$$

The diagonal coherent Green function $F_{i\sigma}(i\omega_l)$ and the off-diagonal one $F'_{ij\sigma}(i\omega_l)$ in Eqs. (10)–(13) are defined, respectively, by

$$F_{i\sigma}(i\omega_l)=(g^{-1}-\Sigma)^{-1}_{il\sigma il\sigma}, \quad (14)$$

$$F'_{ij\sigma}(i\omega_l)=(g^{-1}-\Sigma)^{-1}_{il\sigma jl\sigma}(1-\delta_{ij}). \quad (15)$$

The dynamical CPA neglects the intersite dynamical interaction energy ΔE. The free energy is then given by

$$\mathcal{F}_{\mathrm{CPA}}=\tilde{\mathcal{F}}-\sum_i \beta^{-1}\ln\int\delta\xi_i\delta\eta_i e^{-\beta E^{(i)}[\xi_i,\eta_i]}. \quad (16)$$

The coherent potential $\Sigma_{i\sigma}(i\omega_l)$ is determined in such a way that the effect of ΔE becomes as small as possible. This yields the condition

$$\langle\tilde{t}_i\rangle\equiv\frac{\int\delta\xi_i\delta\eta_i\tilde{t}_i e^{-\beta E^{(i)}[\xi_i,\eta_i]}}{\int\delta\xi_i\delta\eta_i e^{-\beta E^{(i)}[\xi_i,\eta_i]}}=0. \quad (17)$$

The above equation is also written as

$$\langle G_{i\sigma}(i\omega_l,i\omega_l)\rangle=F_{i\sigma}(i\omega_l), \quad (18)$$

$$G_{i\sigma}(i\omega_l,i\omega_l)=[(F_i^{-1}-\delta v_i)^{-1}]_{il\sigma il\sigma}. \quad (19)$$

Here $\langle G_{i\sigma}(i\omega_l,i\omega_l)\rangle$ at the left-hand side (lhs) is the impurity Green function in the effective medium, which is derived from the impurity Hamiltonian in the effective medium defined by[30]

$$\hat{H}^{(i)}(\tau)=\tilde{H}(\tau)+U_i n_{i\uparrow}(\tau)n_{i\downarrow}(\tau)-\int_0^{\beta}d\tau'\sum_{\sigma}a^{\dagger}_{i\sigma}(\tau)\Sigma_{i\sigma}(\tau-\tau')a_{i\sigma}(\tau'), \quad (20)$$

$$\tilde{H}(\tau)=\sum_{j,\sigma}(\epsilon_j^0-\mu-h_j\sigma)n_{j\sigma}(\tau)+\sum_{i,j,\sigma}t_{ij}a^{\dagger}_{i\sigma}(\tau)a_{j\sigma}(\tau)+\sum_{j,\sigma}\int_0^{\beta}d\tau' a^{\dagger}_{j\sigma}(\tau)\Sigma_{j\sigma}(\tau-\tau')a_{j\sigma}(\tau'). \quad (21)$$

Since $\langle G_{i\sigma}(i\omega_l,i\omega_l)\rangle$ is the temperature Green function for the impurity Hamiltonian in the effective medium,[31] the coherent potential $\Sigma_{i\sigma}(i\omega_l)$ is the self-energy of the system in the single-site approximation.

Note that the CPA equation (18) is also obtained from the stationary condition

$$\frac{\delta \mathcal{F}_{\mathrm{CPA}}}{\kappa_\sigma(i\omega_l)\,\delta\Sigma_\sigma(i\omega_l)} = \beta^{-1}[F_{i\sigma}(i\omega_l) - \langle G_{i\sigma}(i\omega_l, i\omega_l)\rangle] = 0. \tag{22}$$

Here $\kappa_\sigma(i\omega_l) = 1 - F_{i\sigma}(i\omega_l)^{-2}\,\delta F_{i\sigma}(i\omega_l)/\delta\Sigma_\sigma(i\omega_l)$.

Equation (17) or (18) determines the coherent potential, therefore, the free energy. The difficulty in the dynamical CPA approach is in calculating the average impurity Green function in Eq. (18) as well as the impurity energy (10). We adopted in our previous paper[19] the Monte Carlo (MC) method to implement the dynamical CPA. Although it is exact in principle, the MC method needs a large amount of computing time to obtain quantitative results in particular at low temperatures. We propose in the next section simpler but more analytic method.

Before we proceed to the next step, we rewrite the free energy (16) by means of the effective potential projected onto the zero-frequency variables $\xi = \xi_{i0}$ and $\eta = \eta_{i0}$,

$$\mathcal{F}_{\mathrm{CPA}} = \tilde{\mathcal{F}} - \beta^{-1}\ln \int \sqrt{\frac{\beta U}{4\pi}}\, d\xi \sqrt{\frac{\beta U}{4\pi}}\, d\eta e^{-\beta E(\xi,\eta)}. \tag{23}$$

Here we have redefined $\mathcal{F}_{\mathrm{CPA}}$ and $\tilde{\mathcal{F}}$ by those per site assuming that all the sites are equivalent to each other. Moreover, here and in the following we omit all the site indices for simplicity.

The effective potential $E(\xi,\eta)$ consists of the static energy $E_{\mathrm{st}}(\xi,\eta)$ and the dynamical one. The latter describes all the dynamical effects.

$$E(\xi,\eta) = E_{\mathrm{st}}(\xi,\eta) + E_{\mathrm{dyn}}(\xi,\eta), \tag{24}$$

$$E_{\mathrm{st}}(\xi,\eta) = -\beta^{-1}\mathrm{tr}\,\ln(1-\delta v_0 F) + \frac{1}{4}U(\eta^2+\xi^2), \tag{25}$$

$$e^{-\beta E_{\mathrm{dyn}}(\xi,\eta)} = \overline{D_\uparrow D_\downarrow} = \int \left[\prod_{l=1}^{\infty} \frac{\beta U}{2\pi} d^2\xi_l \frac{\beta U}{2\pi} d^2\eta_l\right] D_\uparrow D_\downarrow \times \exp\left[-\frac{\beta U}{2}\sum_{l=1}^{\infty}(|\eta_l|^2 + |\xi_l|^2)\right], \tag{26}$$

$$D_\sigma = \det[\,\delta_{lm} - \tilde{v}_\sigma(i\omega_l - i\omega_m)\tilde{g}_\sigma(i\omega_m)]. \tag{27}$$

Here δv_0 in Eq. (25) is defined by $\delta v_\sigma(0) = v_\sigma(0) - \Sigma_\sigma(i\omega_l)$. The upper bar in Eq. (26) denotes the Gaussian average with respect to all the field variables with finite frequencies. $\tilde{v}_\sigma(i\omega_l)$ in the determinant D_σ is the dynamical potential without the zero-frequency part, and $\tilde{g}_\sigma(i\omega_l)$ is the static Green function on an impurity site.

$$\tilde{v}_\sigma(i\omega_l) = v_\sigma(i\omega_l) - v_\sigma(0)\,\delta_{l0}, \tag{28}$$

$$\tilde{g}_\sigma(i\omega_l) = [F_\sigma(i\omega_l)^{-1} - \delta v_\sigma(0)]^{-1}. \tag{29}$$

The variational principle (22) for the free energy (23) is then written as

$$\frac{\delta \mathcal{F}_{\mathrm{CPA}}}{\kappa_\sigma(i\omega_l)\,\delta\Sigma_\sigma(i\omega_l)} = \beta^{-1}\left\langle\left\langle F_\sigma(i\omega_l) - \tilde{g}_\sigma(i\omega_l) + \beta\frac{\delta E_{\mathrm{dyn}}(\xi,\eta)}{\kappa_\sigma(i\omega_l)\,\delta\Sigma_\sigma(i\omega_l)}\right\rangle\right\rangle_{\mathrm{eff}} = 0. \tag{30}$$

Therefore, we obtain the expression of the impurity Green function in the medium as

$$\langle G_{i\sigma}(i\omega_l, i\omega_l)\rangle = \left\langle \tilde{g}_\sigma(l) - \beta\frac{\delta E_{\mathrm{dyn}}(\xi,\eta)}{\kappa_\sigma(i\omega_l)\,\delta\Sigma_\sigma(i\omega_l)}\right\rangle_{\mathrm{eff}}. \tag{31}$$

Here $\langle\sim\rangle_{\mathrm{eff}}$ means the classical average with respect to the effective potential $E(\xi,\eta)$.

The neglect of the dynamical potential $E_{\mathrm{dyn}}(\xi,\eta)$ is called the static approximation. In the static approximation, the present theory reduces to the single-site spin fluctuation theory by Hubbard[7] and Hasegawa.[8] The static approximation becomes exact in the atomic limit because the charge and spin operators (n_i and m_i) commute with the Hamiltonian there, and it also becomes exact in the high-temperature limit because the time dependence of the field variables $\xi_i(\tau)$ and $\eta_i(\tau)$ are negligible in the limit. Furthermore, the static approximation yields the Hartree-Fock approximation at the ground state, which is correct in the weak Coulomb-interaction limit. In the intermediate region, however, one has to take into account the dynamical potential $E_{\mathrm{dyn}}(\xi,\eta)$ in general.

III. HARMONIC APPROXIMATION TO DYNAMICAL CPA

A. Harmonic approximation and its thermodynamics

The difficulty in obtaining the dynamical correction originates in the determinant of the scattering matrix given by Eq. (27). We expand here the determinant with respect to the frequency modes of the dynamical potential $\tilde{v}_\sigma(i\omega_\nu)$ as

$$D_\sigma = 1 + \sum_\nu (D_{\nu\sigma} - 1) + \sum_{(\nu,\nu')} (D_{\nu\nu'\sigma} - D_{\nu\sigma} - D_{\nu'\sigma} + 1) + \cdots, \tag{32}$$

$$D_{\nu\sigma} = \det[\,\delta_{lm} - [\tilde{v}_\sigma(i\omega_\nu)\,\delta_{l-m,\nu} + \tilde{v}_\sigma(i\omega_{-\nu})\,\delta_{l-m,-\nu}]\tilde{g}_\sigma(i\omega_m)], \tag{33}$$

$$D_{\nu\nu'\sigma} = \det[\,\delta_{lm} - [\tilde{v}_\sigma(i\omega_\nu)\,\delta_{l-m,\nu} + \tilde{v}_\sigma(i\omega_{-\nu})\,\delta_{l-m,-\nu}]\tilde{g}_\sigma(i\omega_m) - [\tilde{v}_\sigma(i\omega_{\nu'})\,\delta_{l-m,\nu'} + \tilde{v}_\sigma(i\omega_{-\nu'})\,\delta_{l-m,-\nu'}]\tilde{g}_\sigma(i\omega_m)]. \tag{34}$$

The first term in Eq. (32) corresponds to the zeroth approximation (i.e., the static approximation), the second term expresses the independent scattering due to each dynamical potential $v_\sigma(i\omega_\nu)$, and the higher-order terms express the mode-mode couplings. We neglect here these mode-mode

coupling terms and only take into account the independent frequency terms. This is called the harmonic approximation.[21,22]

The approximation is exactly up to the second order in U in the weak Coulomb interaction region.

$$\exp[-\beta E_{\rm dyn}(\xi,\eta)]=1+U^2\sum_{\nu=1}^{\infty}\tilde{c}^{(1)}_{\nu\uparrow}\tilde{c}^{(1)}_{\nu\downarrow}+\cdots, \quad (35)$$

$$\tilde{c}^{(1)}_{\nu\sigma}=\frac{1}{\beta}\sum_{l=-\infty}^{\infty}\tilde{g}_{\sigma}(l-\nu)\tilde{g}_{\sigma}(l). \quad (36)$$

Here and in the followings, we express $i\omega_l$ as l for simplicity. In the strong Coulomb interaction region, it has been shown numerically that the harmonic approximation quantitatively reproduces the Kondo susceptibility obtained by the renormalization group approach,[32] when it is applied to the Anderson model.[27] More important is the fact that the approximation is independent of the strength of the Coulomb interaction. Therefore, the harmonic approximation is considered to be suitable for the description of the intermediate region where a variety of interesting phenomena occur in the condensed matters.

The determinant $D_{\nu\sigma}$ in the harmonic approximation is written by the product of those of tridiagonal matrices as follows.[22]

$$D_{\nu\sigma}=D_{\nu\sigma}(0)D_{\nu\sigma}(1)\cdots D_{\nu\sigma}(\nu-1), \quad (37)$$

$$D_{\nu\sigma}(k)=\begin{vmatrix} \ddots & & & & & & \\ & 1 & 1 & & 0 & & \\ & a_{-\nu+k\sigma}(\nu) & 1 & 1 & & & \\ & & a_{k\sigma}(\nu) & 1 & 1 & & \\ & & & a_{\nu+k\sigma}(\nu) & 1 & 1 & \\ & 0 & & & a_{2\nu+k\sigma}(\nu) & & \\ & & & & & \ddots & \end{vmatrix}. \quad (38)$$

Here $D_{\nu\sigma}(k)$ is the determinant of the tridiagonal matrix consisting of the Green functions with the frequency remainder k for the modulus ν, and $a_{n\sigma}(\nu)$ is defined by

$$a_{n\sigma}(\nu)=\tilde{v}_{\sigma}(\nu)\tilde{v}_{\sigma}(-\nu)\tilde{g}_{\sigma}(n-\nu)\tilde{g}_{\sigma}(n). \quad (39)$$

Note that according to the Laplace expansion theorem $D_{\nu\sigma}(k)$ is expressed by the determinants of the submatrices as

$$D_{\nu\sigma}(k)=D^{(0)}_{\nu\sigma}(\nu,k)D^{(0)}_{\nu\sigma}(-\nu,k)-a_{k\sigma}(\nu)D^{(1)}_{\nu\sigma}(\nu,k)D^{(1)}_{\nu\sigma}(-\nu,k), \quad (40)$$

$$D^{(m)}_{\nu\sigma}(\nu',k)=\begin{vmatrix} 1 & 1 & & 0 & \\ a_{(m+1)\nu'+k\sigma}(\nu) & 1 & 1 & & \\ & a_{(m+2)\nu'+k\sigma}(\nu) & 1 & 1 & \\ & & a_{(m+3)\nu'+k\sigma}(\nu) & 1 & 1 \\ & & & & \ddots \\ 0 & & & & \end{vmatrix}. \quad (41)$$

The determinant $D^{(m)}_{\nu\sigma}(\pm\nu,k)$ is expanded as follows (see Appendix A).

$$D^{(m)}_{\nu\sigma}(\pm\nu,k)=\sum_{n=0}^{\infty}(-)^n[\tilde{v}_{\sigma}(\nu)\tilde{v}_{\sigma}(-\nu)]^nA^{(m)}_{n\pm\nu k\sigma}. \quad (42)$$

Here

$$A^{(m)}_{0\pm\nu k\sigma}\equiv 1, \quad (43)$$

$$A^{(m)}_{n\pm\nu k\sigma}=\sum_{l_1=m+1}^{\infty}\sum_{l_2=m+1}^{l_1-2}\cdots\sum_{l_n=m+1}^{l_{n-1}-2}\hat{a}_{l_1(\pm\nu)+k\sigma}(\nu)\times\hat{a}_{l_2(\pm\nu)+k\sigma}(\nu)\cdots\hat{a}_{l_n(\pm\nu)+k\sigma}(\nu), \quad (44)$$

and

$$\hat{a}_{n\sigma}(\nu)=\tilde{g}_{\sigma}(n-\nu)\tilde{g}_{\sigma}(n). \quad (45)$$

Substituting Eq. (42) for $m=0$ and 1 into Eq. (40), we obtain an expression of $D_{\nu\sigma}(k)$ with respect to the dynamical potential as follows:

$$D_{\nu\sigma}(k)=\sum_{l=0}^{\infty}\frac{1}{l!}\left(\frac{i\beta\tilde{v}_{\sigma}(\nu)\tilde{v}_{\sigma}(-\nu)}{2\pi\nu}\right)^{l}B_{\nu\sigma}^{(l)}(k). \quad (46)$$

Here

$$B_{\nu\sigma}^{(0)}(k)\equiv 1, \quad (47)$$

$$B_{\nu\sigma}^{(l)}(k)=(-)^{l}l!\left(\frac{2\pi\nu}{i\beta}\right)^{l}\Bigg[A_{l\nu k\sigma}^{(0)}+\sum_{m=0}^{l-1}(A_{m\nu k\sigma}^{(0)}A_{l-m-\nu k\sigma}^{(0)}+\hat{a}_{k\sigma}A_{m\nu k\sigma}^{(1)}A_{l-1-m-\nu k\sigma}^{(1)})\Bigg]. \quad (48)$$

Therefore, we obtain the expansion form of $D_{\nu\sigma}$ from Eqs. (37) and (46) as follows.

$$D_{\nu\sigma}=\sum_{l=0}^{\infty}\frac{1}{l!}(4\beta\tilde{v}_{\sigma}(\nu)\tilde{v}_{\sigma}(-\nu))^{l}\left(\frac{i}{8\pi\nu}\right)^{l}B_{\nu\sigma}^{(l)}, \quad (49)$$

$$B_{\nu\sigma}^{(l)}=\sum_{\sum_{k=0}^{\nu-1}l_k=l}\frac{l!}{\left[\prod_{k=0}^{\nu-1}l_k!\right]}\left[\prod_{k=0}^{\nu-1}B_{\nu\sigma}^{(l_k)}(k)\right]. \quad (50)$$

The dynamical potential is obtained by substituting the first and second terms of Eq. (32) into Eq. (26).

$$e^{-\beta E_{\rm dyn}(\xi,\eta)}=\left[1+\sum_{\nu=1}^{\infty}(\overline{D}_{\nu\uparrow}-1)\right]\left[1+\sum_{\nu=1}^{\infty}(\overline{D}_{\nu\downarrow}-1)\right]+\sum_{\nu=1}^{\infty}\overline{\delta D_{\nu\uparrow}\delta D_{\nu\downarrow}}. \quad (51)$$

Here $\delta D_{\nu\sigma}=D_{\nu\sigma}-\overline{D}_{\nu\sigma}$. $\overline{D}_{\nu\sigma}$ and $\overline{D_{\nu\uparrow}D_{\nu\downarrow}}$ are calculated from Eq. (49) by using the Gaussian integrals, so that we obtain $\overline{D}_{\nu\sigma}=1$ and

$$\overline{D_{\nu\uparrow}D_{\nu\downarrow}}=\sum_{l=0}^{\infty}U^{2l}\left(\frac{i}{2\pi\nu}\right)^{2l}B_{\nu\uparrow}^{(l)}B_{\nu\downarrow}^{(l)}. \quad (52)$$

Therefore, Eq. (51) yields the following expression of the dynamical potential.

$$E_{\rm dyn}(\xi,\eta)=-\frac{1}{\beta}\ln\left[1+\sum_{\nu=1}^{\infty}(\overline{D_{\nu\uparrow}D_{\nu\downarrow}}-1)\right]. \quad (53)$$

The impurity Green function is obtained from Eqs. (31) and (53) as

$$\langle G_{\sigma}(l,l)\rangle=\langle G_{\sigma}^{(\rm eff)}(\xi,\eta,l)\rangle_{\rm eff}, \quad (54)$$

$$G_{\sigma}^{(\rm eff)}(\xi,\eta,l)=\tilde{g}_{\sigma}(l)+\frac{\sum_{\nu=1}^{\infty}\frac{\delta(\overline{D_{\nu\uparrow}D_{\nu\downarrow}})}{\kappa_{\sigma}(l)\,\delta\Sigma_{\sigma}(l)}}{1+\sum_{\nu=1}^{\infty}(\overline{D_{\nu\uparrow}D_{\nu\downarrow}}-1)}, \quad (55)$$

$$\frac{\delta(\overline{D_{\nu\uparrow}D_{\nu\downarrow}})}{\kappa_{\sigma}(l)\,\delta\Sigma_{\sigma}(l)}=\sum_{l'=1}^{\infty}U^{2l'}\left(\frac{i}{2\pi\nu}\right)^{2l'}B_{\nu-\sigma}^{(l')}\frac{\delta B_{\nu\sigma}^{(l')}}{\kappa_{\sigma}(l)\,\delta\Sigma_{\sigma}(l)}. \quad (56)$$

Here $G_{\sigma}^{(\rm eff)}(\xi,\eta,l)$ is the effective impurity Green function projected onto the static field variables.

The first term on the right-hand side (rhs) of Eq. (55) is the static Green function and the second term is the dynamical correction. Note that the second term vanishes in the $U\rightarrow 0$ limit as it should be. Furthermore, it also vanishes in the atomic limit because $\overline{D_{\nu\uparrow}D_{\nu\downarrow}}$ does not depend on $\Sigma_{\sigma}(l)$ there.

The CPA equation (18) is then expressed as

$$\langle G_{\sigma}^{(\rm eff)}(\xi,\eta,l)\rangle_{\rm eff}=F_{\sigma}(l), \quad (57)$$

$$F_{\sigma}(l)=\int\frac{\rho(\epsilon)d\epsilon}{i\omega_l-\Sigma_{\sigma}(l)-\epsilon}. \quad (58)$$

Here $\rho(\epsilon)$ is the density of states (DOS) in the noninteracting system described by H_0.

Equations (23), (24), (53), and (57) completely determine the thermodynamics of the system. The local charge and magnetic moment are obtained by taking the derivatives, $\partial\mathcal{F}_{\rm CPA}/\partial\epsilon_0$ and $-\partial\mathcal{F}_{\rm CPA}/\partial h$ as

$$\langle n\rangle=\langle i\eta\rangle_{\rm eff}, \quad (59)$$

$$\langle m\rangle=\langle\xi\rangle_{\rm eff}. \quad (60)$$

The amplitudes of charge and local moments are calculated from $\langle n\rangle\pm 2\langle n_{\uparrow}n_{\downarrow}\rangle$ and $\partial\mathcal{F}_{\rm CPA}/\partial U=\langle n_{\uparrow}n_{\downarrow}\rangle$,

$$\langle n^2\rangle=\langle n\rangle-\frac{1}{2}\langle\eta^2\rangle_{\rm eff}-\frac{1}{2}\langle\xi^2\rangle_{\rm eff}+\frac{2}{\beta U}+2\left\langle\left[\frac{\partial E_{\rm dyn}}{\partial U}\right]_{v}\right\rangle_{\rm eff}, \quad (61)$$

$$\langle m^2\rangle=\langle n\rangle+\frac{1}{2}\langle\eta^2\rangle_{\rm eff}+\frac{1}{2}\langle\xi^2\rangle_{\rm eff}-\frac{2}{\beta U}-2\left\langle\left[\frac{\partial E_{\rm dyn}}{\partial U}\right]_{v}\right\rangle_{\rm eff}. \quad (62)$$

Here $[\ ]_v$ means taking the derivative fixing the static potential $v_{\sigma}(0)$, and is given by

$$\left[\frac{\partial E_{\rm dyn}}{\partial U}\right]_{v}=-\frac{1}{\beta}\frac{\sum_{\nu=1}^{\infty}\left[\frac{\partial(\overline{D_{\nu\uparrow}D_{\nu\downarrow}})}{\partial U}\right]_{v}}{1+\sum_{\nu=1}^{\infty}(\overline{D_{\nu\uparrow}D_{\nu\downarrow}}-1)}, \quad (63)$$

$$\left[\frac{\partial(\overline{D_{\nu\uparrow}D_{\nu\downarrow}})}{\partial U}\right]_{v}=\sum_{l=1}^{\infty}2lU^{2l}\left(\frac{i}{2\pi\nu}\right)^{2l}B_{\nu\uparrow}^{(l)}B_{\nu\downarrow}^{(l)}. \quad (64)$$

The entropy is obtained from $\beta^2 \partial \mathcal{F}_{\rm CPA}/\partial\beta$ as

$$S=\beta^2\frac{\partial\tilde{\mathcal{F}}}{\partial\beta}+\left\langle \beta^2\frac{\partial E}{\partial\beta}\right\rangle -1 + \ln\int\left[\sqrt{\frac{\beta U}{4\pi}}\,d\xi\sqrt{\frac{\beta U}{4\pi}}\,d\eta\right]e^{-\beta(E(\xi,\eta)-\langle E\rangle_{\rm eff})}, \tag{65}$$

$$\beta^2\frac{\partial\tilde{\mathcal{F}}}{\partial\beta}=-2\int d\epsilon\rho(\epsilon)[\{1-f(\epsilon)\}\ln\{1-f(\epsilon)\} + f(\epsilon)\ln f(\epsilon)]+\sum_{l,\sigma}\int d\epsilon\rho(\epsilon)\left[\ln\left(1-\frac{\Sigma_\sigma(l)}{i\omega_l-\epsilon}\right) + \frac{i\omega_l\Sigma_\sigma(l)}{(i\omega_l-\epsilon)[i\omega_l-\Sigma_\sigma(l)-\epsilon]}\right], \tag{66}$$

$$\left\langle\beta^2\frac{\partial E}{\partial\beta}\right\rangle_{\rm eff}=\left\langle\sum_{l\sigma}\ln[1-\delta v_\sigma(0)F_\sigma(l)]\right\rangle_{\rm eff} + \left\langle\ln\left(1+\sum_{\nu=1}^{\infty}(\overline{D_{\nu\uparrow}D_{\nu\downarrow}}-1)\right)\right\rangle_{\rm eff} + \left\langle\frac{\sum_{\nu=1}^{\infty}\beta\left[\frac{\partial\overline{D_{\nu\uparrow}D_{\nu\downarrow}}}{\partial\beta}\right]_{\omega\Sigma}}{1+\sum_{\nu=1}^{\infty}(\overline{D_{\nu\uparrow}D_{\nu\downarrow}}-1)}\right\rangle_{\rm eff}. \tag{67}$$

Here Eq. (66) denotes the contribution from the coherent self-energy as well as the entropy of noninteracting electrons. $f(\epsilon)$ denotes the Fermi distribution function. The first term in Eq. (67) expresses the contribution from the static impurity potential, the second and the third terms are the contributions of the dynamical potential. Note that $[\partial\overline{D_{\nu\uparrow}D_{\nu\downarrow}}/\partial\beta]_{\omega\Sigma}$ means to take the derivative fixing the frequency $i\omega_l$ and the coherent potential $\Sigma_\sigma(l)$. The last term in Eq. (65) produces the magnetic entropy when the local moment is well defined.

The thermodynamic energy is obtained from the relation $F+\beta^{-1}S$ as

$$\langle H-\mu N\rangle=\frac{1}{\beta}\sum_{l,\sigma}i\omega_l F_\sigma(l)+\frac{1}{4}U\left[\langle\eta^2\rangle_{\rm eff}-\frac{2}{\beta U}+\langle\xi^2\rangle_{\rm eff} - \frac{2}{\beta U}\right]-\left\langle\frac{\sum_{\nu=1}^{\infty}\left[\frac{\partial\overline{D_{\nu\uparrow}D_{\nu\downarrow}}}{\partial\beta}\right]_{\omega\Sigma}}{1+\sum_{\nu=1}^{\infty}(\overline{D_{\nu\uparrow}D_{\nu\downarrow}}-1)}\right\rangle_{\rm eff}. \tag{68}$$

Here the first term on the rhs is the coherent contribution of the kinetic energy, the second one corresponds to the double counting term in the Hartree-Fock energy, the last term is the dynamical correction in the single-site approximation.

B. Asymptotic approximation

The key term to implement the theoretical framework presented in the last subsection is the dynamical correction $\overline{D_{\nu\uparrow}D_{\nu\downarrow}}$, which is calculated from $B^{(l)}_{\nu\sigma}$ [Eq. (50)] or $B^{(l)}_{\nu\sigma}(k)$ [Eq. (48)]. The number of terms in $A^{(m)}_{n\nu k\sigma}$ from which $B^{(l)}_{\nu\sigma}(k)$'s are calculated, however, exponentially increases with increasing n, as seen from Eq. (44), which makes the actual calculations impossible. We, therefore, develop an approximate calculation scheme in this section.

Note that the determinants $\{D^{(m)}_{\nu\sigma}(\pm\nu,k)\}$ $(m=0,1)$ defined by Eq. (41) have the following recursive relation as is verified by using Laplace's expansion theorem.

$$D^{(0)}_{\nu\sigma}(\pm\nu,k)=D^{(1)}_{\nu\sigma}(\pm\nu,k)-a_{\pm\nu+k\sigma}(\nu)D^{(2)}_{\nu\sigma}(\pm\nu,k), \tag{69}$$

$$D^{(1)}_{\nu\sigma}(\pm\nu,k)=D^{(2)}_{\nu\sigma}(\pm\nu,k)-a_{2(\pm\nu)+k\sigma}(\nu)D^{(3)}_{\nu\sigma}(\pm\nu,k), \tag{70}$$

$$\cdots$$

$$D^{(m)}_{\nu\sigma}(\pm\nu,k) = D^{(m+1)}_{\nu\sigma}(\pm\nu,k)-a_{(m+1)(\pm\nu)+k\sigma}(\nu)D^{(m+2)}_{\nu\sigma}(\pm\nu,k). \tag{71}$$

The determinant $D^{(m)}_{\nu\sigma}(\pm\nu,k)$ consists of the static Green functions $\{\tilde{g}_\sigma(l)\}$ with the frequency $|l|$ higher than $|m\nu|$. This means that one may replace $D^{(m)}_{\nu\sigma}(\pm\nu,k)$ with an approximate determinant $\tilde{D}^{(m)}_{\nu\sigma}(\pm\nu,k)$, which becomes exact in the asymptotically large $|m|$ limit.

$$D^{(m)}_{\nu\sigma}(\pm\nu,k)\approx\tilde{D}^{(m)}_{\nu\sigma}(\pm\nu,k). \tag{72}$$

Such an approximate form $\tilde{D}^{(m)}_{\nu\sigma}(\pm\nu,k)$ is obtained as follows. The coherent potential $\Sigma_\sigma(l)$ reduces to the Hartree-Fock value $\langle v_\sigma(0)\rangle_{\rm eff}$ in the large $|l|$ limit, therefore, the static impurity Green function behaves as $\tilde{g}_\sigma(l)\sim 1/i\omega_l$ for large $|l|$. In this region, we have the following relations

$$\tilde{g}_\sigma((l-1)\nu+k)\tilde{g}_\sigma(l\nu+k) \sim\frac{\beta}{2\pi i\nu}[\tilde{g}_\sigma((l-1)\nu+k)-\tilde{g}_\sigma(l\nu+k)], \tag{73}$$

$$\tilde{g}_\sigma((l-2)\nu+k)\tilde{g}_\sigma((l-1)\nu+k)\tilde{g}_\sigma(l\nu+k) \sim\frac{1}{2}\frac{\beta}{2\pi i\nu}[\tilde{g}_\sigma((l-2)\nu+k)\tilde{g}_\sigma((l-1)\nu+k) -\tilde{g}_\sigma((l-1)\nu+k)\tilde{g}_\sigma(l\nu+k)]. \tag{74}$$

Successive application of the above relations to $\{A^{(m)}_{n\nu k\sigma}\}$ yields the following relations.

$$A^{(m)}_{1\nu k\sigma}\sim\frac{\beta}{2\pi i\nu}\tilde{g}_\sigma(m\nu+k), \tag{75}$$

$$A^{(m)}_{2\nu k\sigma} \sim \frac{1}{2}\left(\frac{\beta}{2\pi i\nu}\right)^2 \tilde{g}_\sigma(m\nu+k)\tilde{g}_\sigma((m+1)\nu+k). \quad (76)$$

Repeating the same procedure, we obtain the asymptotic form $\tilde{D}^{(m)}_{\nu\sigma}(\pm\nu,k)$ as follows.

$$\tilde{D}^{(m)}_{\nu\sigma}(\pm\nu,k) = \sum_{n=0}^{\infty} (-)^n [\tilde{v}_\sigma(\nu)\tilde{v}_\sigma(-\nu)]^n \tilde{A}^{(m)}_{n\nu k\sigma}, \quad (77)$$

$$\tilde{A}^{(m)}_{n\nu k\sigma} = \frac{1}{n!}\left(\frac{\beta}{2\pi i\nu}\right)^n \tilde{g}_\sigma(m\nu+k) \times \tilde{g}_\sigma((m+1)\nu+k)\cdots\tilde{g}_\sigma((m+n-1)\nu+k), \quad (78)$$

$$\tilde{A}^{(m)}_{n-\nu k\sigma} = \frac{1}{n!}\left(\frac{\beta}{-2\pi i\nu}\right)^n \tilde{g}_\sigma((m+1)(-\nu)+k) \times \tilde{g}_\sigma((m+2)(-\nu)+k)\cdots\tilde{g}_\sigma((m+n)(-\nu)+k). \quad (79)$$

Here we defined $\tilde{A}^{(m)}_{0\pm\nu k\sigma}=1$. We call the approximation (72) the mth-order asymptotic approximation.

Explicit forms of $D^{(0)}_{\nu\sigma}(\pm\nu,k)$ and $D^{(1)}_{\nu\sigma}(\pm\nu,k)$ in the asymptotic approximation are obtained from Eqs. (69)–(71) and (77). Substituting $D^{(0)}_{\nu\sigma}(\pm\nu,k)$ and $D^{(1)}_{\nu\sigma}(\pm\nu,k)$ into Eq. (40), we obtain the asymptotic form of $D_{\nu\sigma}(k)$ and, therefore, that of $B^{(l)}_{\nu\sigma}(k)$ as follows:

$$\tilde{D}_{\nu\sigma}(k) = \sum_{l=0}^{\infty}\frac{1}{l!}\left(\frac{i\beta\tilde{v}_\sigma(\nu)\tilde{v}_\sigma(-\nu)}{2\pi\nu}\right)^l \tilde{B}^{(l)}_{\nu\sigma}(k). \quad (80)$$

Here $\tilde{B}^{(0)}_{\nu\sigma}(k)=1$ and $\tilde{B}^{(l)}_{\nu\sigma}(k)$ for $l>0$ is given by

$$\tilde{B}^{(l)}_{\nu\sigma}(k) = b^{(0)}_{l\sigma}(\nu,k) + \sum_{m=0}^{l-1}(-)^{l-m}\binom{l}{m} \times\left[b^{(0)}_{m\sigma}(\nu,k)b^{(0)}_{l-m\sigma}(-\nu,k) + \frac{2\pi(l-m)\nu}{i\beta} \times\tilde{g}_\sigma(-\nu+k)\tilde{g}_\sigma(k)b^{(1)}_{m\sigma}(\nu,k)b^{(1)}_{l-m-1\sigma}(-\nu,k)\right]. \quad (81)$$

The functions $b^{(0)}_{m\sigma}(\pm\nu,k)$ and $b^{(1)}_{m\sigma}(\pm\nu,k)$ in the zeroth-order and the second-order asymptotic approximation are presented in Appendix B.

The dynamical correction $\overline{D_{\nu\uparrow}D_{\nu\downarrow}}$ in the asymptotic approximation is given by Eq. (52) in which $B^{(l)}_{\nu\sigma}$ has been replaced by its asymptotic form $\tilde{B}^{(l)}_{\nu\sigma}$.

$$\overline{\tilde{D}_{\nu\uparrow}\tilde{D}_{\nu\downarrow}} = \sum_{l=0}^{\infty} U^{2l}\left(\frac{i}{2\pi\nu}\right)^{2l}\tilde{B}^{(l)}_{\nu\uparrow}\tilde{B}^{(l)}_{\nu\downarrow}. \quad (82)$$

Here $\tilde{B}^{(l)}_{\nu\sigma}$ is defined by Eq. (50) with $B^{(l)}_{\nu\sigma}(k)$ replaced by $\tilde{B}^{(l)}_{\nu\sigma}(k)$.

The asymptotic approximation becomes exact irrespective of m when it is applied to the Anderson model with a wide conduction band because the relations (73) and (74) exactly hold true for the noninteracting Anderson impurity Green function on the upper complex plane.[21] Such a dynamical correction has yielded a reasonable description in the Kondo limit.[27] Therefore, we expect that even the zeroth-order asymptotic approximation can describe reasonably the physical properties in the strongly correlated region. In fact, the Green function $\tilde{g}_\sigma(n)$ is expanded in the atomic region, where the transfer integrals are small as compared with the Coulomb interaction, as follows.

$$\tilde{g}_\sigma(n) = \frac{1}{i\omega_n - v_\sigma(0) - \dfrac{M_2}{i\omega_n - \Sigma_\sigma(n)} + \cdots}. \quad (83)$$

Here M_2 is the second moment defined by $M_2 = \int \epsilon^2\rho(\epsilon)d\epsilon$, which is comparable to W^2, W being the bandwidth for noninteracting system.

The condition that the asymptotic approximation holds true, therefore, is given by $|i\omega_n - \langle v_\sigma(0)\rangle_{\rm eff}|^2 \gg M_2$. In the case of the half-filled band, it reduces to

$$\omega_n^2 + U^2 \gg W^2 \ (n>m). \quad (84)$$

Therefore, one can expect that the asymptotic approximation is valid for the strong Coulomb interaction region; $U/W \gg 1$ or for the high-temperature region; $T/W \gg 1$ even if $m \sim 1$. When m is increased, Eq. (84) is satisfied at smaller Coulomb interaction or lower temperatures. This means that the asymptotic approximation is suitable either in the strongly correlated region or in the high-temperature region.

C. Interpolation theory

The asymptotic approximation to the dynamical potential is an approach from a large U/W or T/W limit. Therefore, it is not easy to describe the dynamical effects in the region of small U/W or small T/W. We propose here a simple interpolation scheme that is valid in both weak and strong Coulomb interaction limits.

The idea basic to finding such a unified scheme is that both the dynamical correction in the original harmonic approximation and that in the asymptotic approximation have the same form; equations (52) and (82) are expanded in a series of U in the same way. Only their coefficients $\{B^{(l)}_{\nu\uparrow}B^{(l)}_{\nu\downarrow}\}$ are different each other. Because the mth asymptotic approximation is not expected to be valid for small Coulomb interaction U, we replace the coefficients $\{\tilde{B}^{(l)}_{\nu\uparrow}\tilde{B}^{(l)}_{\nu\downarrow}\}$ up to the $2l$th order with the original ones,

$$\overline{D_{\nu\uparrow}D_{\nu\downarrow}} = \sum_{n=0}^{l} U^{2n}\left(\frac{i}{2\pi\nu}\right)^{2n} B^{(n)}_{\nu\uparrow}B^{(n)}_{\nu\downarrow} + \sum_{n=l+1}^{\infty} U^{2n}\left(\frac{i}{2\pi\nu}\right)^{2n}\tilde{B}^{(n)}_{\nu\uparrow}\tilde{B}^{(n)}_{\nu\downarrow}. \quad (85)$$

Here the first few terms of $B^{(n)}_{\nu\sigma}$ are given as follows:

$$B^{(0)}_{\nu\sigma} = 1, \quad (86)$$

$$B^{(1)}_{\nu\sigma}=\frac{2\pi i\nu}{\beta}\sum_{l=0}^{\infty}[\tilde{g}_\sigma(l-\nu)\tilde{g}_\sigma(l)+\tilde{g}_\sigma(l+\nu)^*\tilde{g}_\sigma(l)^*], \tag{87}$$

$$B^{(2)}_{\nu\sigma}=\left(\frac{2\pi\nu}{\beta}\right)^2\mathrm{Re}\Bigg[2\sum_{l=0}^{\infty}\tilde{g}_\sigma(l-\nu)\tilde{g}_\sigma(l)[\tilde{g}_\sigma(l-2\nu)\tilde{g}_\sigma(l-\nu)+\tilde{g}_\sigma(l-\nu)\tilde{g}_\sigma(l)+\tilde{g}_\sigma(l)\tilde{g}_\sigma(l+\nu)]-\sum_{l=0}^{\nu-1}[\tilde{g}_\sigma(l-\nu)\tilde{g}_\sigma(l)]^2\Bigg]+B^{(1)2}_{\nu\sigma}. \tag{88}$$

We call the approximation (85) the $(2l,m)$ asymptotic approximation. It should be noted that one can control the accuracy of the dynamical correction increasing either $2l$ or m, or increasing both $2l$ and m within the harmonic approximation.

In the application of the theory to the magnetism, the spin fluctuations are more important in most cases. We may neglect the thermal charge fluctuations in such a case using the local saddle-point approximation to the static-charge field η. The free energy (23) is then given by

$$\mathcal{F}_{\mathrm{CPA}}=\tilde{\mathcal{F}}-\beta^{-1}\ln\int\sqrt{\frac{\beta U}{4\pi}}\,d\xi e^{-\beta E_{\mathrm{eff}}(\xi)}, \tag{89}$$

$$E_{\mathrm{eff}}(\xi)=E_{\mathrm{st}}(\xi)+E_{\mathrm{dyn}}(\xi). \tag{90}$$

Here $E_{\mathrm{st}}(\xi)=E_{\mathrm{st}}(\xi,\eta^*)$ and $E_{\mathrm{dyn}}(\xi)=E_{\mathrm{dyn}}(\xi,\eta^*)$ with Eq. (85). η^* is the saddle-point value defined by

$$i\eta^*=n(\xi)=\frac{1}{\beta}\sum_{l,\sigma}G^{(\mathrm{eff})}_\sigma(\xi,\eta^*(\xi),l). \tag{91}$$

Furthermore, we adopt the decoupling approximation to the CPA equation (57) that is correct up to the second moment,

$$\sum_{q=\pm1}\frac{1}{2}\left(1+q\frac{\langle\xi\rangle_{\mathrm{eff}}}{x}\right)[G^{(\mathrm{eff})}_\sigma(\xi,\eta^*(\xi),l)]_{\xi=qx}=F_\sigma(l). \tag{92}$$

Here $x=\sqrt{\langle\xi^2\rangle_{\mathrm{eff}}}$, and $[\ ]_{\xi=qx}$ means taking the value at $\xi=qx$. Note that the classical averages $\langle\sim\rangle_{\mathrm{eff}}$ here and in the followings are taken with respect to the energy $E_{\mathrm{eff}}(\xi)$.

The local charge and moment derived from Eq. (89) are given by

$$\langle n\rangle=\langle n(\xi)\rangle_{\mathrm{eff}}, \tag{93}$$

$$\langle m\rangle=\langle\xi\rangle_{\mathrm{eff}}. \tag{94}$$

The expressions of the amplitudes of the charge and local moment, (61) and (62), are replaced by

$$\langle n^2\rangle=\langle n\rangle+\frac{1}{2}\langle n(\xi)^2\rangle_{\mathrm{eff}}-\frac{1}{2}\left(\langle\xi^2\rangle_{\mathrm{eff}}-\frac{2}{\beta U}\right)+2\left\langle\left[\frac{\partial E_{\mathrm{dyn}}(\xi)}{\partial U}\right]_v\right\rangle_{\mathrm{eff}}, \tag{95}$$

$$\langle m^2\rangle=\langle n\rangle-\frac{1}{2}\langle n(\xi)^2\rangle_{\mathrm{eff}}+\frac{1}{2}\left(\langle\xi^2\rangle_{\mathrm{eff}}-\frac{2}{\beta U}\right)-2\left\langle\left[\frac{\partial E_{\mathrm{dyn}}(\xi)}{\partial U}\right]_v\right\rangle_{\mathrm{eff}}. \tag{96}$$

The entropy derived from Eq. (89) is given by

$$S=\beta^2\frac{\partial\tilde{\mathcal{F}}}{\partial\beta}+\left\langle\beta^2\frac{\partial E_{\mathrm{eff}}(\xi)}{\partial\beta}\right\rangle_{\mathrm{eff}}-\frac{1}{2}+\ln\int\left[\sqrt{\frac{\beta U}{4\pi}}d\xi\right]e^{-\beta(E_{\mathrm{eff}}(\xi)-\langle E_{\mathrm{eff}}(\xi)\rangle_{\mathrm{eff}})}. \tag{97}$$

The first and second terms at the rhs are given by Eqs. (66) and (67) with the saddle-point value η^*. The thermodynamic energy is given by Eq. (68) in which $\langle\eta^2\rangle_{\mathrm{eff}}-2/\beta U$, the second term at the rhs, has been replaced by $-\langle n(\xi)^2\rangle_{\mathrm{eff}}$. All the other expressions are the same as before except that η has been replaced by its saddle point value η^*.

In the simplified calculation scheme, $\langle\xi\rangle_{\mathrm{eff}}$ and $x=\sqrt{\langle\xi^2\rangle_{\mathrm{eff}}}$ have to be determined self-consistently; (1) we start from a set of input values $\langle\xi\rangle_{\mathrm{eff}}$, x, and $[v_\sigma(0)](\xi=\pm x)$ (i.e., $\epsilon_0-\mu+U[n(\pm x)\mp x\sigma]/2$), (2) calculate the dynamical coherent potential $\Sigma_\sigma(l)$ solving Eq. (92), (3) under the medium $\Sigma_\sigma(l)$, obtain $n(\xi)$ solving the saddle-point equation (91) for each ξ, (4) calculate the effective potential $E_{\mathrm{eff}}(\xi)$ [Eq. (90)], (5) determine the chemical potential according to Eq. (93), (6) calculate a new set of $\langle\xi\rangle_{\mathrm{eff}}$, x, and $[v_\sigma(0)](\xi=\pm x)$. The steps (1)–(6) are repeated until the self-consistency is achieved.

IV. NUMERICAL EXAMPLE

We present in this section the numerical results of our model calculations obtained by the dynamical CPA. Bearing in mind Fe and Ni showing both localized and itinerant behaviors in their magnetism, we consider here two cases: (1) the electron number $n=1.44$ $(=7.2/5)$, the Coulomb interaction $2U/W=2.289$, and the bcc noninteracting DOS, (2) $n=1.80$ $(=9.0/5)$, $2U/W=3.429$, and the fcc noninteracting DOS. The same sets of input parameters have been used in our previous investigations with use of the VA.[11] All the numerical calculations have been done on the level of the (4, 2) asymptotic approximation. The ν-frequency sum in the dynamical potential (53) has been taken into account up to $\nu_{\max}=100$, and the sum of U expansion in Eq. (85) has been taken up to $n_{\max}=16$. The matsubara frequency sums such as Eqs. (25), (68), and (91) show a slow convergence and an oscillation with increasing the number of terms. We, therefore, adopted the random phase method that we devised (see Appendix. C).

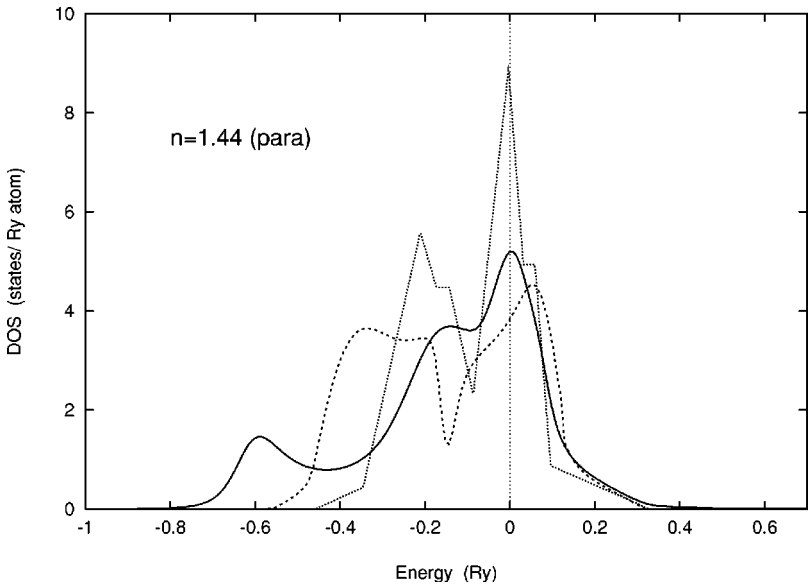

FIG. 1. Calculated densities of states (DOS) of the single-particle excitations in the dynamical CPA (solid curve) and the static approximation (dashed curve) for the bcc Fe in the paramagnetic state, which is defined by the electron number $n=1.44$, the Coulomb interaction $2U/W=2.289$, the temperature $2T/W=0.0281$, and the noninteracting density of states shown by the dotted curve. The bandwidth W is chosen to be 0.45 Ry for convenience.

Figure 1 shows the average DOS in the paramagnetic state for Fe [i.e., case (1)]. The single-particle DOS for the dynamical CPA was calculated by the Padé numerical analytic continuation.[33] The DOS in the static approximation show the bonding-antibonding structure and the band broadening due to thermal static spin fluctuations. The dynamical effects suppress such an excess band broadening and create a satellite peak at -0.6 Ry as seen in Fig. 1. The main band around the Fermi level shows the narrowing by 20% when it is compared with the noninteracting DOS. This feature is also found in the recent ground-state calculations with use of the quantum chemical approach and the Mori-Zwanzig projection technique,[34] and is considered to remain even above T_C because the related energy scale U is much higher than T_C, although the satellite peak in the paramagnetic state is not found in Fe experimentally.[35]

In the ferromagnetic state with a large exchange splitting, the dynamical effects on the DOS become less important as shown in Fig. 2, because the electron-hole excitations are suppressed. The static approximation forms the three-peak structure that is well understood by the simple Stoner model and the noninteracting DOS presented in Fig. 1. On the other hand, the main peak of the upspin DOS in the correlated electrons is split into two peaks and the weight of the peak around $\omega=-0.45$ Ry is enhanced (see the dashed curve in Fig. 2). Note that the dynamical effects on the downspin band are much less than those for the upspin band. This feature seems to stabilize the ferromagnetism. The resulting total DOS shows a band narrowing by about 10% as compared with that of the static approximation or the Stoner model, which seems to be consistent with the photoemission data of Fe.[35,36]

Various calculated effective potentials of Fe in the paramagnetic state are presented in Fig. 3. It is remarkable that the effective potential with dynamical correlations shows a single minimum at $\xi=0$, while the static potential shows the double minima at $\xi=\pm 0.46\mu_B$, because the dynamical potential shows a deep minimum at $\xi=0$ and saturate at $\xi=$

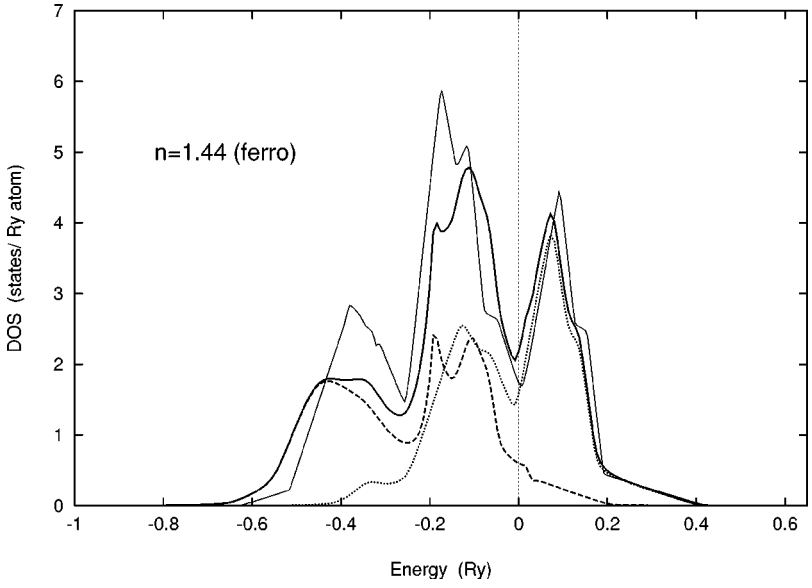

FIG. 2. Calculated DOS in the dynamical CPA for the ferromagnetic Fe at $2T/W=0.007\,04$. Full curve: the total DOS, dashed curve: the upspin DOS, dotted curve: the downspin DOS. The total DOS in the static approximation is shown by the thin solid curve.

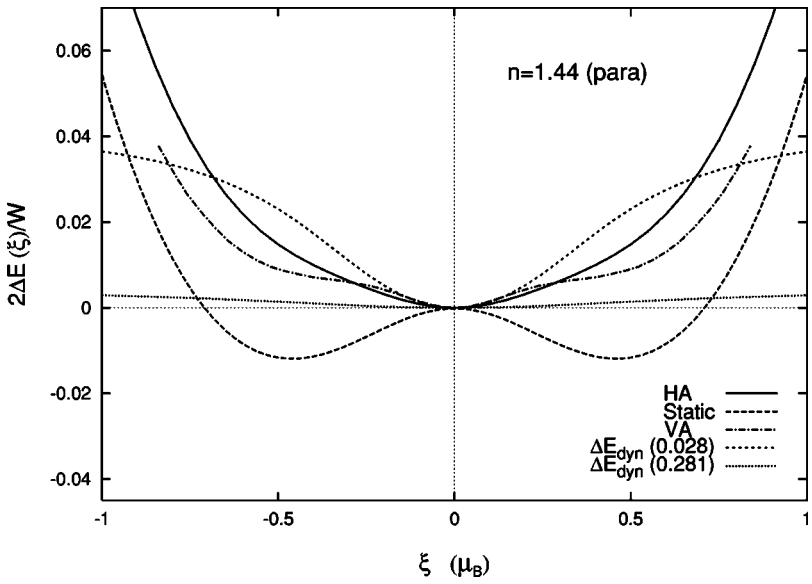

FIG. 3. Effective potentials of the paramagnetic Fe in the dynamical CPA (solid curve), the static approximation (dashed curve), and the variational approach (VA) (dot-dashed curve) which are calculated at $2T/W=0.0281$, $2T/W=0.0281$, and $2T/W=0.009\,84$, respectively. The dynamical contributions $E_{\rm dyn}$ at $2T/W=0.0281$ and $2T/W=0.281$ are also given by dotted curves. All the curves are shifted so that they are zero at $\xi=0$.

$\pm\infty$. The results qualitatively agree with that of the VA,[11] which was determined by using the variational principle to the effective potential and the Gutzwiller-type ground-state theory. The basic difference between the present theory and the VA is that the latter adiabatically takes into account the ground-state energy, while the former takes into account the nonadiabatic effects automatically. In fact, the dynamical potential in the present theory becomes small when the temperature $2T/W$ is increased as shown in Fig. 3, and finally the effective potential reduces to that of the static approximation in the high-temperature limit. In the ferromagnetic state, the effective potential becomes asymmetric due to the ferromagnetic molecular field from the surrounding polarized spins, and show a minimum at $\xi=0.49\mu_{\rm B}$ (see Fig. 4). Note that the effective potential in the VA has also the same feature, although it has a shallower minimum because of the stronger dynamical correction in the VA. The effective potential in the static approximation shows a double minimum structure even in the ferromagnetic state, although it has the minimum at $\xi=0.51\mu_{\rm B}$.

We have calculated the magnetic moments and susceptibilities for Fe self-consistently at each temperature. The results are presented in Fig. 5. The magnetization in the static approximation takes the value $m_0=0.511(=2.56/5)\ \mu_{\rm B}$ at $T=0$, and gradually decrease with increasing temperature. The calculated Curie temperature is $2T_C/W=0.0253$ ($T_C=900$ K for $W=0.45$ Ry). In the dynamical CPA, we obtained the ground-state magnetization $m_0=0.494\ (=2.47/5)$ by extrapolation to $T=0$ and the Curie temperature $2T_C/W=0.0118$ ($T_C=420$ K for $W=0.45$ Ry), which is smaller than that of the static approximation by a factor of 2. The VA leads to a smaller ground-state magnetization $m_0=0.443\ (2.215/5)\ \mu_{\rm B}$ and a lower Curie temperature $2T_C/W=0.0084$ (300 K for $W=0.45$ Ry). The dynamical result for T_C, which is much smaller than the experimental value 1040 K,[37] is attributed to the strong quantum spin fluctuations in the single-orbital model. The amplitude of local moments are $0.73\mu_{\rm B}$ at $T=0$ for both the static approximation and the dynamical CPA, and hardly change with varying temperature as shown in Fig. 5.

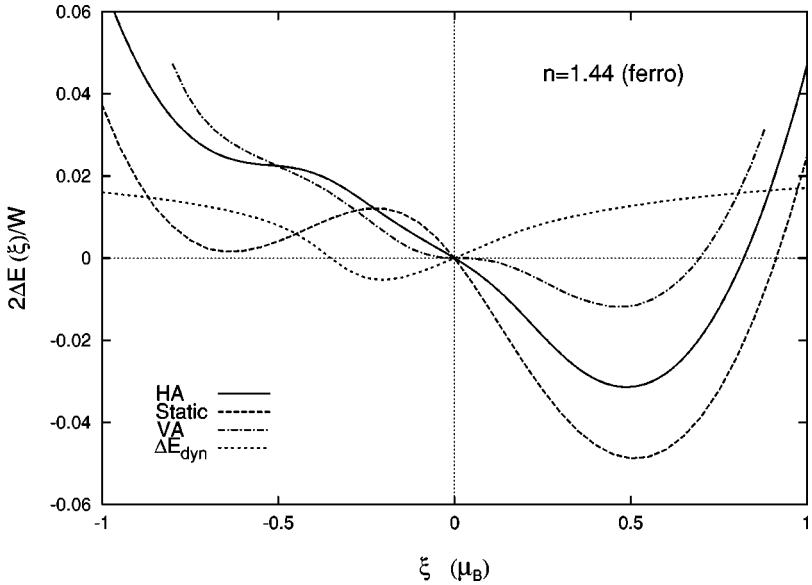

FIG. 4. Effective potentials of the ferromagnetic Fe in the dynamical CPA (solid curve), the static approximation (dashed curve), and the VA (dot-dashed curve) which are calculated at $2T/W=0.004\,22$. The dynamical contribution $E_{\rm dyn}$ is also given by dotted curve.

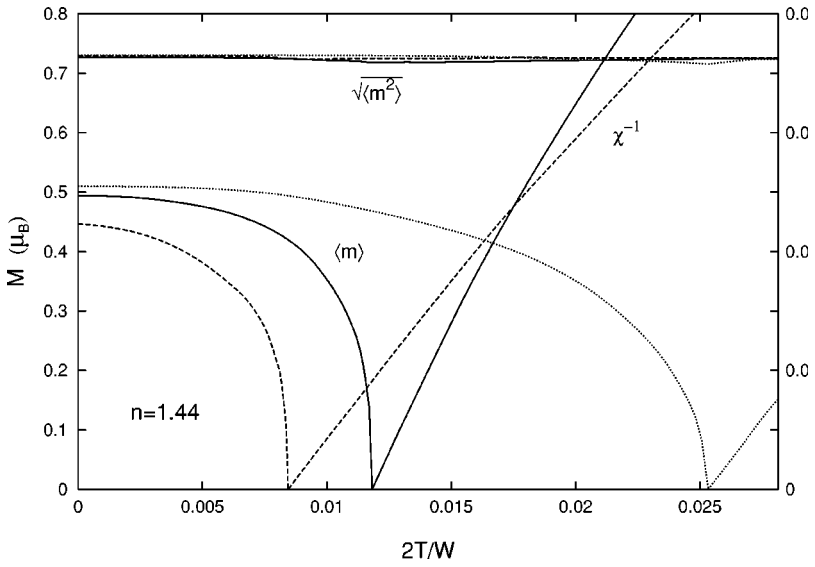

FIG. 5. Magnetization vs temperature curves, the inverse susceptibility curves, and the curves of amplitude of local moments in the bcc Fe obtained by the dynamical CPA (solid curves), the static approximation (dotted curves), and the VA (dashed curves), respectively. The curves below $2T/W=0.003$ in the dynamical CPA were obtained by an extrapolation.

The inverse susceptibilities have been calculated by taking the derivative $\delta(2h/W)/\delta\langle m\rangle$ numerically. Both the static approximation and the dynamical CPA yield the Curie-Weiss susceptibility. The calculated effective Bohr magneton numbers defined by $\chi^{-1}=3(T-\Theta)/m_{\mathrm{eff}}^2$ are, however, different from each other: $m_{\mathrm{eff}}/m_0=1.75$ (static and VA) and 1.39 (dynamical CPA). The latter is comparable to the experimental value[38] 1.44.

In the case of Ni [i.e., the case (2)], the situation is somewhat different from Fe. We did not find the ferromagnetic solution in the present theory; the dynamical effects make the ferromagnetism unstable. The calculated DOS in the paramagnetic state are presented in Fig. 6. The thermal static spin fluctuations in the static approximation broaden the DOS. The dynamical effects create a satellite peak at $\omega_s=-0.5$ Ry and shrink the main band by about 15% as compared with that of the noninteracting system. These values are in good agreement with the detailed calculations at the ground state.[34,39–41] The experimental satellite peak position and the band narrowing are reported to be $\omega_s=-0.46$ Ry and 25%, respectively.[36,42–44]

Calculated effective potentials show a single minimum for both static and dynamical cases as shown in Fig. 7. The dynamical effects make the effective potential steeper, so that the thermal spin fluctuations are suppressed. It should be noted that the steeper potential is not obtained simply by adding the dynamical potential to the static result; it is obtained by a self-consistent depolarization of medium.

Magnetic moments and susceptibilities for Ni are shown in Fig. 8. In the case of the static approximation we obtain the ground-state magnetization $m_0=0.146\,(=0.730/5)\ \mu_{\mathrm{B}}$ and the Curie temperature $2T_C/W=0.0192$ (530 K for $W=0.35$ Ry), as well as the Curie-Weiss susceptibility with the effective Bohr magneton number $m_{\mathrm{eff}}/m_0=3.2$. The VA also yields the ferromagnetism with $m_0=0.123\mu_{\mathrm{B}}$ and $T_C=0.0156$. However, the dynamical CPA yields the paramagnetic state over all temperatures as seen from the temperature dependence of its inverse susceptibility in Fig. 8. The ampli-

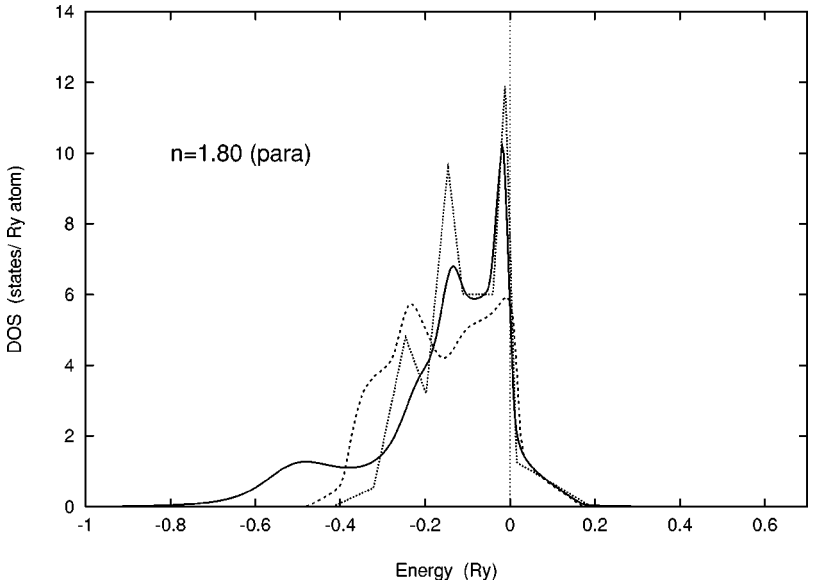

FIG. 6. Calculated densities of states (DOS) in the dynamical CPA (solid curve) and the static approximation (dashed curve) for the fcc Ni in the paramagnetic state, which is defined by $n=1.80$, $2U/W=3.429$, $2T/W=0.0362$. The noninteracting density of states shown by the dotted curve. The bandwidth W is chosen to be 0.35 Ry for convenience.

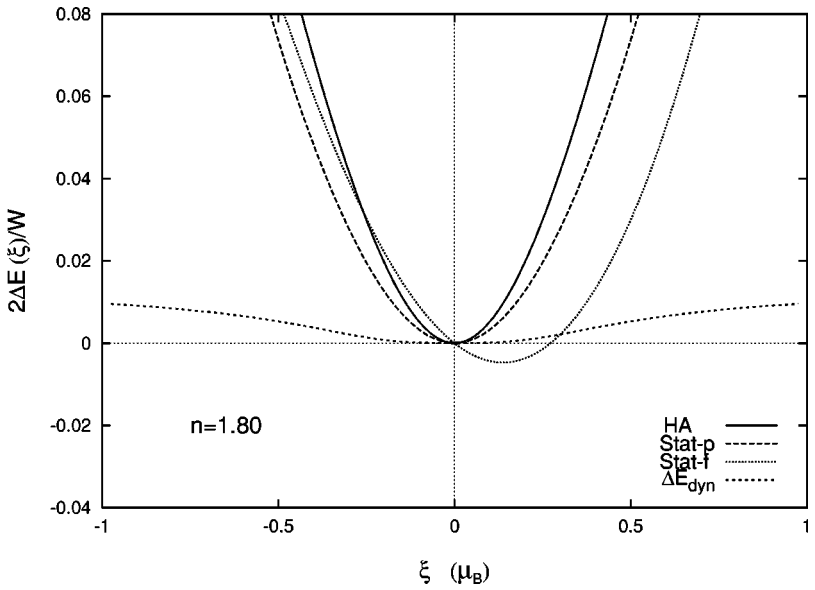

FIG. 7. Effective potentials of the paramagnetic Ni in the dynamical CPA (solid curve) and the static approximation (dashed curve) that are calculated at $2T/W=0.0362$. The dynamical contribution E_{dyn} at the same temperature, and the static potential in the ferromagnetic state at $2T/W=0.003\,62$ are also given by dotted curves. All the curves are shifted so that they are zero at $\xi=0$.

tudes of local moments being extrapolated to $T=0$ is $\sqrt{\langle m^2\rangle}(T=0)=0.464\mu_{\mathrm{B}}$, which is enhanced by 6% as compared with the static case, $\sqrt{\langle m^2\rangle}(T=0)=0.437\mu_{\mathrm{B}}$.

Although it has not been clarified yet quantitatively under what condition the ferromagnetism is stabilized on the fcc lattice in the single-band model, the present result of the paramagnetism for Ni is quite conceivable because the calculated DOS is consistent with those of the ground-state calculations and because the condition to the ferromagnetism becomes very severe in general in the low-density region.[10,16,45] Recent Monte Carlo calculations of the Hubbard model based on the dynamical mean-field theory[46] also showed the paramagnetism for $n=1.8$ and the intermediate U values when only the nearest-neighbor hoppings are taken into account on the fcc lattice. In our previous VA calculations, the local electron correlations were treated by means of the local ansatz[14] that describes best the correlations in rather weak Coulomb interaction region by means of the local operator $O_i=(n_{i\uparrow}-\langle n_{i\uparrow}\rangle)(n_{i\downarrow}-\langle n_{i\downarrow}\rangle)$. The local ansatz tends to stabilize the magnetic state excessively in the large U limit when the electron number deviates from the half-filled. Ni might be the case because of large $2U/W(=3.429)$. The Hilbert space has to be expanded more carefully in such a strongly correlated electron system (see Chap. 5 in Ref. 1, for example).

V. SUMMARY

We have developed the dynamical CPA to the correlated electron system on the basis of the functional integral method and the HA (harmonic approximation). The theory describes the electron correlations at finite temperatures by means of the coherent potential put over all the lattice sites and the dynamical impurity potential embedded in the medium. The latter was treated within the HA that takes into account all the single-mode dynamical scatterings, and the former is determined so that the temperature Green function on the impurity site becomes identical to the coherent one,

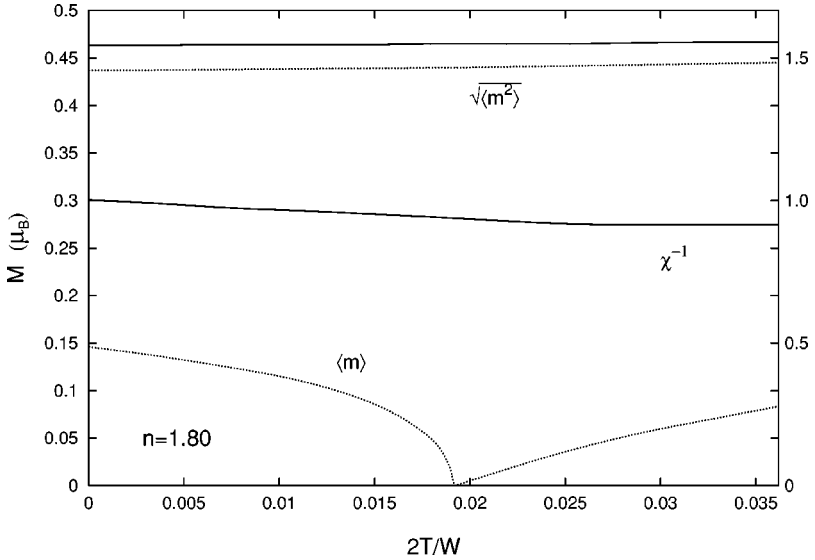

FIG. 8. Magnetization vs temperature curves, the inverse susceptibility curves, and the curves of amplitude of local moments in Ni obtained by the dynamical CPA (solid curves) and the static approximation (dotted curves), respectively. The curves below $2T/W=0.005$ in the dynamical CPA were obtained by an extrapolation.

which is called the CPA. We have proposed an approximate calculation scheme to the dynamical potential called the $(2l, m)$ asymptotic approximation, which uses the correct results of the HA up to $2l$th order in U and replaces the higher-order terms by means of those in the mth asymptotic approximation.

The present theory becomes accurate in the high-temperature limit, reproduces exactly the free energy up to the second order in the small U limit, and describes quantitatively the physical quantities in the strong-U limit within the single-site approximation. There is no need to adopt a statistical method such as Monte Carlo sampling to obtain the coherent potential (i.e., the self-energy), so that one can easily obtain the single-particle DOS using the Padé analytic continuation to the self-energy. Moreover, there is a clear relation between the present theory and the single-site spin fluctuation theory by Hubbard and Hasegawa that the former reduces to the latter when the dynamical part of the former theory is neglected.

We have performed the model calculations to the bcc Fe and the fcc Ni using the sets of parameters employed in the previous VA calculations. Numerical results for Fe in the (4, 2) asymptotic approximation showed that the dynamical effects reduce the Curie temperature by a factor of 2, and yield a Curie Weiss susceptibility with an effective Bohr magneton number that is smaller than that of the static approximation by 20%. The calculated amplitude of the local moment is found to be close to that of the static approximation and hardly changes with varying temperature. In the case of Ni, we found that the dynamical effects make the ferromagnetism unstable. The amplitude of local moment is enhanced by 6% due to the dynamical correlations. We found in both cases that the dynamical CPA creates a satellite peak in the single-particle DOS in the paramagnetic state. The band narrowing due to the correlations are found to be 20% (10%) in the paramagnetic (ferromagnetic) state in the bcc Fe, and 15% in the case of Ni. These results are consistent with the recent ground-state calculations. In the case of the ferromagnetic Fe, the DOS calculated by the dynamical CPA does not show any clear satellite structure but shows a band narrowing by about 10%. This feature is consistent with the photoemission data.

The single-band model to the bcc Fe and the fcc Ni certainly overestimates the quantum fluctuations; it yields too small a T_C (420 K for $W=0.45$ Ry) in the case of Fe, and yields the paramagnetism in the case of Ni. Taking into account the *s*, *p*, *d* orbitals and realistic band structure, we expect the Curie temperatures $T_C \sim 1500$ K for Fe and $T_C \sim 1000$ K for Ni. The interatomic spin fluctuations as described by Eq. (12) should reduce the Curie temperature to the experimental values (1040 K for Fe and 630 K for Ni). To realize such a scenario, further developments of the dynamical CPA towards the realistic description of the magnetic properties are highly desired.

ACKNOWLEDGMENTS

The author would like to express his sincere thanks to Professor Peter Fulde for valuable discussions and a critical reading of the manuscript. He is also grateful to Dr. N. Shannon for correcting the manuscript. Numerical calculations have been done partly with use of the facilities of the Supercomputer Center, Institute for Solid State Physics, University of Tokyo.

APPENDIX A: DERIVATION OF EQ. (42)

Let us consider the determinant of a finite matrix as follows.

$$D^{(m,M)}=\begin{vmatrix} 1 & 1 & & & 0 & & \\ a_{(m+1)\nu+k} & 1 & & 1 & & & \\ & a_{(m+2)\nu+k} & & 1 & 1 & & \\ & & & a_{(m+3)\nu+k} & 1 & 1 & \\ & & & & & \ddots & \\ 0 & & & & & & \\ & & & & & a_{M\nu+k} & 1 \end{vmatrix}. \tag{A1}$$

By using the Laplace expansion, we have the recursion relation as

$$D^{(m,M)}=D^{(m,M-1)}-a_{M\nu+k}D^{(m,M-2)}. \tag{A2}$$

In the same way, we obtain the following recursion relations in general.

$$D^{(m,n)}=D^{(m,n-1)}-a_{n\nu+k}D^{(m,n-2)}, \tag{A3}$$

$$D^{(m,m+1)}=1-a_{(m+1)\nu+k}, \tag{A4}$$

$$D^{(m,m)}=1. \tag{A5}$$

Now, we start from the following identity:

$$D^{(m,M)}=1+\sum_{l_1=m+1}^{M}(D^{(m,l_1)}-D^{(m,l_1-1)}). \tag{A6}$$

Substituting Eq. (A3) into Eq. (A6), we obtain

$$D^{(m,M)}=1-\sum_{l_1=m+1}^{M}a_{l_1\nu+k}D^{(m,l_1-2)}. \tag{A7}$$

Repeating the same procedure for $D^{(m,l_1-2)}$, we have

$$D^{(m,M)}=1-\sum_{l_1=m+1}^{M}a_{l_1\nu+k}\left(1-\sum_{l_2=m+1}^{l_1-2}a_{l_2\nu+k}D^{(m,l_2-2)}\right), \tag{A8}$$

and finally we reach the following expansion.

$$D^{(m,M)}=1+\sum_{n=1}^{M}(-)^n\sum_{l_2=m+1}^{l_1-2}\cdots\sum_{l_n=m+1}^{l_{n-1}-2}a_{l_1\nu+k}\cdots a_{l_n\nu+k}. \tag{A9}$$

Substituting $a_n=\tilde{v}_\sigma(\nu)\tilde{v}_\sigma(-\nu)\tilde{g}_\sigma(n-\nu)\tilde{g}_\sigma(n)$ into Eq. (A9) and taking the limit $M\to\infty$, we obtain Eq. (42).

APPENDIX B: $b^{(0)}_{n\sigma}(\nu,k)$ AND $b^{(1)}_{n\sigma}(\nu,k)$ IN THE ZEROTH AND SECOND-ORDER ASYMPTOTIC APPROXIMATION

$B^{(l)}_{\nu\sigma}(k)$ in the asymptotic approximation is obtained from the functions $\{b^{(0)}_{n\sigma}(\pm\nu,k)\}$ and $\{b^{(1)}_{n\sigma}(\pm\nu,k)\}$ $(0\leqslant n\leqslant l)$ as shown in Eq. (81).

In the zeroth-order asymptotic approximation, these functions are given by

$$b^{(0)}_{n\sigma}(\nu,k)=p_{\nu k\sigma}(0,n-1), \tag{B1}$$

$$b^{(0)}_{n\sigma}(-\nu,k)=p_{-\nu k\sigma}(1,n), \tag{B2}$$

$$b^{(1)}_{n\sigma}(\nu,k)=p_{\nu k\sigma}(1,n), \tag{B3}$$

$$b^{(1)}_{n\sigma}(-\nu,k)=p_{-\nu k\sigma}(2,n+1). \tag{B4}$$

Here

$$p_{\nu k\sigma}(l,m)=\begin{cases}\left[\prod_{n=l}^{m}\tilde{g}_\sigma(n\nu+k)\right] & (m\geqslant l)\\ 1 & (m<l).\end{cases} \tag{B5}$$

In the second-order asymptotic approximation, they are given by

$$b^{(0)}_{n\sigma}(\nu,k)=p_{\nu k\sigma}(2,n)\left[\tilde{g}_\sigma((n+1)\nu+k)-\frac{2\pi n\nu}{i\beta}\tilde{g}_\sigma(\nu+k)\{\tilde{g}_\sigma(k)+\tilde{g}_\sigma((n+1)\nu+k)\}\right], \tag{B6}$$

$$b^{(0)}_{n\sigma}(-\nu,k)=p_{-\nu k\sigma}(3,n+1)\left[\tilde{g}_\sigma((n+2)(-\nu)+k)+\frac{2\pi n\nu}{i\beta}\tilde{g}_\sigma(2(-\nu)+k)\{\tilde{g}_\sigma(-\nu+k)+\tilde{g}_\sigma((n+2)(-\nu)+k)\}\right], \tag{B7}$$

$$b^{(1)}_{n\sigma}(\nu,k)=p_{\nu k\sigma}(2,n+1)\left[1-\frac{2\pi n\nu}{i\beta}\tilde{g}_\sigma(\nu+k)\right], \tag{B8}$$

$$b^{(1)}_{n\sigma}(-\nu,k)=p_{-\nu k\sigma}(3,n+2)\left[1+\frac{2\pi n\nu}{i\beta}\tilde{g}_\sigma(-2\nu+k)\right]. \tag{B9}$$

APPENDIX C: RANDOM-PHASE TECHNIQUE FOR FREQUENCY SUM

Let us consider the local charge [see Eq. (91)] for simplicity. It is obtained from the following summation.

$$n(\xi)=\frac{2}{\beta}\,\mathrm{Re}\sum_\sigma\sum_{l=0}^{L}e^{i\omega_l\zeta}G^{(\mathrm{eff})}_\sigma(\xi,\eta,l). \tag{C1}$$

Here L is an infinitely large positive integer, and ζ is an infinitesimally small, positive number. The phase factor $\exp(i\omega_l\zeta)$ is essential to the numerical calculation, although we omitted it in the equations in the text for simplicity. It was introduced to obtain the correct operator ordering leading to Eq. (5), and is necessary to hold the equations derived from the free energy.[28] In fact, in the case of $U=0$, Eq. (C1) reduces to the usual relation between the charge and the temperature Green function for noninteracting system. The relation does not hold true if we neglect the phase factor, because in that case we have an additional contribution from the integral along a semicircle contour on the Re $z<0$ plane when we express the rhs of Eq. (C1) by means of the contour integral on the complex plane.

In the numerical calculations, we choose a large but finite integer L and a small but finite number ζ, and take the sum of Eq. (C1). Such a calculation generally yields very slow and oscillating convergence as a function of L. The oscillation and its phase are caused by the small ζ that is not related to the final value $n(\xi)$. We, therefore, introduce a very small Gaussian random number ζ with the average value ζ_0 and standard deviation $s(\ll\zeta_0)$, and average Eq. (C1) over all ζ. Such a superposition cancels the long-range oscillations each other, and yields

$$n(\xi)=\frac{2}{\beta}\,\mathrm{Re}\sum_\sigma\sum_{l=0}^{L}\exp\left(i\omega_l\zeta_0-\frac{1}{2}s^2\omega_l^2\right)G^{(\mathrm{eff})}_\sigma(\xi,\eta,l). \tag{C2}$$

Because of the damping factor $\exp(-s^2\omega_l^2/2)$ in the above expression, we obtain a rapid convergence of the frequency sum.

[1] See, for example, P. Fulde, *Electron Correlations in Molecules and Solids* (Springer, Berlin, 1995), Chap. 11.
[2] M. Cyrot, J. Phys. (Paris) **33**, 25 (1972).
[3] R.L. Stratonovich, Dokl. Akad. Nauk. SSSR **115**, 1097 (1958) [Sov. Phys. Dokl. **2**, 416 (1958)].
[4] J. Hubbard, Phys. Rev. Lett. **3**, 77 (1959).
[5] M.C. Gutzwiller, Phys. Rev. Lett. **10**, 159 (1963).
[6] J. Hubbard, Proc. R. Soc. London, Ser. A **A276**, 238 (1963).
[7] J. Hubbard, Phys. Rev. B **19**, 2626 (1979); **20**, 4584 (1979); **23**, 5974 (1981).
[8] H. Hasegawa, J. Phys. Soc. Jpn. **46**, 1504 (1979); **49**, 178 (1980).
[9] P. Soven, Phys. Rev. **156**, 809 (1967); H. Ehrenreich and L. M. Schwarz, *Solid State Physics*, edited by H. Ehrenreich, F. Seitz, and D. Turnbull (Academic, New York, 1980), Vol. 30.
[10] J. Kanamori, Prog. Theor. Phys. **30**, 275 (1963).
[11] Y. Kakehashi and P. Fulde, Phys. Rev. B **32**, 1595 (1985).
[12] Y. Kakehashi and H. Hasegawa, Phys. Rev. B **36**, 4066 (1987); **37**, 7777 (1988).
[13] Y. Kakehashi, Phys. Rev. B **38**, 6928 (1988).
[14] G. Stollhoff and P. Fulde, Z. Phys. B **29**, 231 (1978); J. Chem. Phys. **73**, 4548 (1980).
[15] H. Hasegawa, J. Phys.: Condens. Matter **1**, 9325 (1990).
[16] G. Kotliar and A.E. Ruckenstein, Phys. Rev. Lett. **57**, 1362 (1986).
[17] Kok-Kwei Pan and Yung-Li Wang, Phys. Rev. B **55**, 2981 (1997).
[18] Yolande H. Szczech, Michael A. Tusch, and David E. Logan, Phys. Rev. Lett. **74**, 2804 (1995).
[19] Y. Kakehashi, Phys. Rev. B **45**, 7196 (1992).
[20] See, for example, *Computational Physics*, edited by K. H. Hoffmann and M. Schreiber (Springer, Berlin, 1996).
[21] D.J. Amit and C.M. Bender, Phys. Rev. B **4**, 3115 (1971).
[22] D.J. Amit and H. Keiter, J. Low Temp. Phys. **11**, 603 (1973).
[23] *Metallic Magnetism*, edited by H. Capellmann, Topics in Current Physics Vol. 42 (Springer-Verlag, Berlin, 1987), Chap. 5.
[24] Y. Kakehashi, Prog. Theor. Phys. **101**, 105 (1990).
[25] *The Magnetism of Amorphous Metals and Alloys*, edited by J. A. Fernandez-Baca and W. Y. Ching (World Scientific, Singapore, 1995), Chap. 1.
[26] Y. Kakehashi, S. Akbar, and N. Kimura, in *Itinerant Electron Magnetism: Fluctuation Effects & Critical Phenomena*, Vol. 55 *of NATO Advanced Study Institute, Series 3: High Technology*, edited by D. Wagner, W. Brauneck, and A. Solontsov (Kluwer Academic, Dordrecht, 1998), p. 193.
[27] Dai Xianxi, J. Phys.: Condens. Matter **3**, 4389 (1991).
[28] W.E. Evanson, J.R. Schrieffer, and S.Q. Wang, J. Appl. Phys. **41**, 1199 (1970); J.R. Schrieffer, W.E. Evanson, and S.Q. Wang, J. Phys. (Paris), Colloq. **32**, C1-1 (1971).
[29] G. Morandi, E. Galleani D'Agliano, F. Napoli, and C.F. Ratto, Adv. Phys. **23**, 867 (1974).
[30] Y. Kakehashi, J. Magn. Magn. Mater. **104-107**, 677 (1992).
[31] D.R. Hamann, Phys. Rev. B **2**, 1373 (1970).
[32] H.R. Krishna-murthy, J.W. Wilkins, and K.G. Wilson, Phys. Rev. B **21**, 1003 (1980).
[33] H.J. Vidberg and J.W. Serene, J. Low Temp. Phys. **29**, 179 (1977).
[34] P. Unger, J. Igarashi, and P. Fulde, Phys. Rev. B **50**, 10 485 (1994).
[35] R.E. Kirby, E. Kisker, F.K. King, and E.L. Garwin, Solid State Commun. **56**, 425 (1985).
[36] D.E. Eastman, F.J. Himpsel, and J.A. Knapp, Phys. Rev. Lett. **44**, 95 (1980).
[37] R. M. Bozorth, *Ferromagnetism* (Van Nostrand, Princeton, 1968).
[38] S. Arajs and R.V. Colvin, J. Phys. Chem. Solids **24**, 1233 (1963).
[39] D.R. Penn, Phys. Rev. Lett. **42**, 921 (1979).
[40] A. Liebsch, Phys. Rev. Lett. **43**, 1431 (1979).
[41] R.H. Victora and L.M. Falicov, Phys. Rev. Lett. **55**, 1140 (1985).
[42] D.E. Eastman, F.J. Himpsel, and J.A. Knapp, Phys. Rev. Lett. **40**, 1514 (1978); F.J. Himpsel, J.A. Knapp, and D.E. Eastman, Phys. Rev. B **19**, 2919 (1979).
[43] W. Eberhardt and E.W. Plummer, Phys. Rev. B **21**, 3245 (1980).
[44] H. Martensson and P.O. Nilsson, Phys. Rev. B **30**, 3047 (1984).
[45] W. Nolting and W. Borgiel, Phys. Rev. B **39**, 6962 (1989).
[46] M. Ulmke, Eur. Phys. J. B **1**, 301 (1998).